

Cessna Citation X Business Aircraft Eigenvalue Stability – Part2: Flight Envelope Analysis

Yamina BOUGHARI¹, Ruxandra Mihaela BOTEZ*¹, Florian THEEL¹,
Georges GHAZI¹

*Corresponding author

¹ETS, Laboratory of Active Controls, Avionics and AeroServoElasticity LARCASE,
1100 Notre Dame West, Montreal, Que., Canada, H3C-1K3,
yamina.boughari.1@ens.etsmtl.ca, Ruxandra.Botez@etsmtl.ca*, f.theel@gmail.com,
georges.ghazi.1@ens.etsmtl.ca

DOI: 10.13111/2066-8201.2017.9.4.5

Received: 21 October 2017/ Accepted: 07 November 2017/ Published: December 2017

Copyright©2017. Published by INCAS. This is an “open access” article under the CC BY-NC-ND license (<http://creativecommons.org/licenses/by-nc-nd/4.0/>)

Abstract: Civil aircraft flight control clearance is a time consuming, thus an expensive process in the aerospace industry. This process has to be investigated and proved to be safe for thousands of combinations in terms of speeds, altitudes, gross weights, Xcg / weight configurations and angles of attack. Even in this case, a worst-case condition that could lead to a critical situation might be missed. To address this problem, models that are able to describe an aircraft's dynamics by taking into account all uncertainties over a region within a flight envelope have been developed using Linear Fractional Representation. In order to investigate the Cessna Citation X aircraft Eigenvalue Stability envelope, the Linear Fractional Representation models are implemented using the speeds and the altitudes as varying parameters. In this paper Part 2, the aircraft longitudinal eigenvalue stability is analyzed in a continuous range of flight envelope with varying parameter of True airspeed and altitude, instead of a single point, like classical methods. This is known as the aeroelastic stability envelope, required for civil aircraft certification as given by the Circular Advisory “Aeroelastic Stability Substantiation of Transport Category Airplanes AC No: 25.629-18”. In this new methodology the analysis is performed in time domain based on Lyapunov stability and solved by convex optimization algorithms by using the linear matrix inequalities to evaluate the eigenvalue stability, which is reduced to search for the negative eigenvalues in a region of flight envelope. It can also be used to study the stability of a system during an arbitrary motion from one point to another in the flight envelope. A whole aircraft analysis results' for its entire envelope are presented in the form of graphs, thus offering good readability, and making them easily exploitable.

Key Words: Eigenvalue Stability, Aeroelastic Stability, Flight Control Clearance, Robustness Analysis

NOMENCLATURE

A, B, C, D	= State space matrices
P	= Positive Definite Matrix
\mathbb{R}	= Real number field
\mathbb{C}	= Complex number field
\mathbb{N}	= Integer number field

A^T	= Transposition of matrix A
A^{-1}	= Inverse of matrix A
A^*	= Transconjugate of matrix A
Θ	= The variation range of each uncertainty

1. INTRODUCTION

The certification of an aircraft is an important and essential step in the process leading to its first flight. To prove that an aircraft is ready to fly, it must meet several criteria required by various agencies such as Transport Canada (TC), the Federal Aviation Administration (FAA), or the European Aviation Safety Agency (EASA); a multitude of flight combinations in terms of center of gravity position, mass, speed, altitude and angle of attack are used. In the same way as in any aircraft design or production process, the Flight Control Laws (FCL) have to be qualified, cleared and certified [1].

Over the last decades, much research has been done to identify the FCLs' clearance criteria [2]-[4].

Some of these criteria have been reformulated as robustness criteria [5]-[10]. The target criteria for the Airbus team, for example, correspond to the aeroelastic stability, turbulence, comfort and maneuver criteria.

All of these criteria have to be evaluated in the full flight envelope, and for all weight and Xcg configurations [11]-[12].

Flight control clearance criteria have become the focus of many studies conducted by universities and industries in the Group for Aeronautical Research and Technology in EUROPE GARTEUR project [1], [13].

These studies were performed mainly on three aircraft fighter models, the High Incidence Research Model with feedback control HIRM+ which is a generic model, the Aero Data Model In Research Environment ADMIRE, and high performance short take off and vertical landing aircraft model called HWEM, which are both realistic models.

However, the flight control clearance criteria analysis results were mainly published for the HIRM+ generic model [1], and suggested adaptations of these criteria to Cessna Citation X civil aircraft.

Due to the lack of access to real flight control clearance data and the availability of the level D Research Aircraft Flight Simulator at our LARCASE laboratory, we have been motivated to investigate its flight control clearance.

Due to the high volume of the flight clearance criteria tasks, the "eigenvalues stability" criterion [14] was selected to be investigated during this present research.

This criterion is applied for a robustness analysis which has been investigated at the LARCASE laboratory on both civil and military aircrafts: the Hawker 800XP, and the HIRM by using the weight functions method [15]-[16].

Normally the stability criterion has been performed on the longitudinal aircraft closed loop model to test the reliability of the flight control in the presence of uncertainties. This criterion seeks for eigenvalues with negative real parts in the aircraft envelope.

To evaluate this criterion, the results have to be checked with those obtained for the natural stability of the aircraft; the eigenvalues for the longitudinal open loop system should therefore be investigated.

Our study focuses on the Cessna Citation X eigenvalue stability analysis by using the data provided by a Level D Research Aircraft Flight Simulator (RAFS). These data were

used to develop both nonlinear and linear models of the airplane for its longitudinal and lateral motions [17], [18].

In article Part 1 the generation of 26 longitudinal LFR models for 12 Xcg and weight configurations were automated for the whole flight envelope by using a new GUI.

The eigenvalue of the flight envelopes were analyzed in this article Part 2 using the robustness and stability analysis toolbox to assess the Cessna Citation X aircraft open loop stability.

The paper is organized as follows: Firstly, presentations of the stability analysis and Lyapunov stability theories are given.

Next, a description of the resolution method followed by a presentation of the stability analysis interface, and the paper ends with the aircraft stability analysis results discussion and conclusions.

2. STABILITY ANALYSIS

After the development and testing of the Graphical User Interface (GUI), the aircraft LFR models could be created easily.

A stability analysis using this interface, that was developed by researchers at the University of Siena within the framework of the project “Clearance of Flight Control Laws Using Optimization” [13], [19], [20] was performed on the 26 LFR models generated for a longitudinal aircraft model for each weight and Xcg location.

Before dealing with the stability analysis, some concepts are introduced on the determination of stability, based on linear algebra, and on the positive or negative condition of a matrix.

A matrix $A \in \mathbb{R}^{n \times n}$ is defined as “positive” if for each vector $x \in \mathbb{R}^n$, the quadratic equation (1) is positive [21].

$$x^T A x \geq 0, \forall x \in \mathbb{R} \quad (1)$$

One of the properties associated with this definition is that the matrix can be defined as “broadly positive” if and only if all its eigenvalues are positive.

If A is positive, then the values of the A spectrum set are all strictly positive. This strictly positivity can be written under the quadratic form as shown in eq. (2):

$$x^T A x > 0, \forall x \in \mathbb{R} \quad (2)$$

2.1 Lyapunov Stability

Next, the Lyapunov stability direct method is presented. Suppose that a system has an equilibrium point x_e .

The system’s measured energy, noted by $V(x)$, always positive, is defined. The steady state is chosen as the origin of the system, i.e., $V(x_e)$.

If the energy evolution in the vicinity of this point is decreasing, $\frac{d}{dt}V(x) < 0$, it means that the system converges to a stable state.

This notion of energy convergence is the basis of the Lyapunov stability theory [22]. A local equilibrium can thus be defined at the point x_e that is associated with a stability condition, as shown in Figure 1.

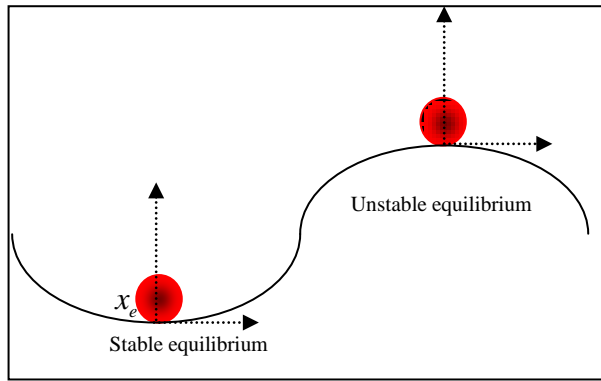


Figure 1. Equilibrium condition

For a system containing uncertainties, that are represented by a parameter vector α , the stability in the asymptotic sense is satisfied if there is a real-value function, and a continuously differentiable $V(x, \alpha)$ such as [22]:

1. $V(0, \alpha) = 0$
2. $V(x, \alpha)_{\|x(t)\| \rightarrow \infty} \rightarrow \infty$
3. $V(x, \alpha) > 0, x \neq 0$
4. $\dot{V}(x, \alpha) < 0, x \neq 0$

2.2 Quadratic Stability

The challenge of this method is to determine the Lyapunov function with the aim to satisfy the system of four eqs. (3). Previous research shown in [23]-[27] focused mainly on the candidate functions shown in the next eq.:

$$V(x, \alpha) = x^T P(\alpha)x \tag{4}$$

with $P > 0, \forall \alpha \in \Theta$

A system is represented by eq. (4) where Θ represents the variations range of each uncertainty, and where P is commonly chosen to be fixed.

If such a function exists, then the system has a “quadratic stability” which is valid for all the uncertain parameters vectors. The robustness of the system is considered to be excellent in such a case.

The Lyapunov function presented in equation (4) gives the required condition for a linear system to be considered “quadratically stable”.

The Lyapunov stability criterion given in eq. (6) lies in the existence of a positive and symmetric definite matrix $P^T = P > 0$ [23]:

$$\dot{x} = Ax \tag{5}$$

$$A^T P = PA < 0 \tag{6}$$

The matrix P is obtained by determining its $\frac{n(n+1)}{2}$ coefficients. The eq. (6) belongs to the class of Linear Matrix Inequalities (LMI). Different toolboxes were developed to automate the resolution process of this type of equations, and to reduce the engineer’s task.

In this paper, the toolbox called YALMIP [28] coupled with the solver SDPT3 ([29], [30]) will be used.

3. RESOLUTION METHOD

In the literature, three different methods can be distinguished by the structure of the Lyapunov function that each one of them chooses. The first method focuses primarily on determining a Lyapunov function constant called Wang-Balakrishnan method [31], while the two other methods focus on dependent parameters functions to refine the solution search; these are Dettori-Scherer [32] and Fu-Dasgupta methods [33]. The Wang-Balakrishnan method was selected to perform the system stability analysis in this paper. The latter is detailed in the following system:

$$\dot{x}(t) = A(\theta)x(t) \quad (7)$$

An uncertain system given by eq. (7) is considered, where x is the state space matrix, $\theta \in \mathbb{R}^{n_\theta}$ is the parameters' vector, and $A \in \mathbb{R}^{n \times n}$ is the aircraft dynamics, and this system can be defined by equations (8) and (9) [19]:

$$A(\theta) = A + B\Delta(\theta)(I - D\Delta(\theta))^{-1} \quad (8)$$

where
$$\Delta(\theta) = \text{diag}(\theta_1 I_{s_1}, \dots, \theta_1 I_{s_1}) \quad (9)$$

An equivalent Linear Fractional Transformation (LFT) of eq. (8) is given by equations (10), (11), and (12) [19]:

$$\dot{x}(t) = Ax(t) + Bu(t) \quad (10)$$

$$y(t) = Cx(t) + Du(t) \quad (11)$$

$$u(t) = \Delta(\theta)y(t) \quad (12)$$

where $u \in \mathbb{R}^d$, $y \in \mathbb{R}^d$, $d = \sum_{i=1}^{n_\theta} s_i$, and A , B , C , D are real matrices of appropriate dimensions.

Matrix A is assumed to be Herwitz type for the stability analysis of the LFR system. Where θ is an uncertain parameter vector, which belongs to Θ a hyper-rectangular with vertices of 2^{n_θ} as $\text{Ver}[\Theta]$, and $\dot{\theta}(t) = 0$ the uncertain parameters that are time invariant. The system of equations is represented by equations (10), (11), and (12) and following conditions are mentioned:

- If there exists a common quadratic Lyapunov function for all matrices $A(\theta)$, where $\theta \in \Theta$, then this function is quadratically stable
- If $A(\theta)$ is Herwitz for all $\theta \in \Theta$, the system is robustly stable.

3.1 Wang-Balakrishnan Method [31]:

The system expressed by eqs. (13), (14), and (15) presents a “quadratic stability”, because its dynamics is given by a symmetric matrix defined as positive: $P \in \mathbb{R}^{n \times n}$, $P = P^T > 0$ and $M \in \mathbb{R}^{d \times d}$, $M = M^T > 0$ as seen in [31]:

$$\begin{bmatrix} A^T P + PA + C^T M C & PB(\theta) + C^T M D(\theta) \\ B(\theta)^T P + D(\theta)^T M C & -M + D(\theta)^T M D(\theta) \end{bmatrix} < 0 \quad (13)$$

where
$$B(\theta) = B\Delta(\theta) \quad (14)$$

and
$$D(\theta) = D\Delta(\theta) \quad (15)$$

Thus, the existence of such matrices can prove with certainty the stability of a system. An alternative to this theorem that uses parameter-dependent Lyapunov functions is given by eqs. (16) and (17); and the demonstration of this theorem is given in detail in [32]:

$$V(x) = x^T Q(\theta)^{-1}x \tag{16}$$

with

$$Q(\theta) = Q_0 + \sum_{j=1}^{n_\theta} \theta_j Q_j \tag{17}$$

4. STABILITY ANALYSIS INTERFACE

In order to accomplish the aircraft eigenvalue stability analysis, a Graphical User Interface is used, which eases and greatly facilitates the analysis task. It offers a wide choice of resolutions via three methods from published research found in [31], [32], and [33]. Figure 2 shows the window with which the user interacts; a brief description of how to manipulate the GUI for the stability analysis is given in the following paragraph. There are two main sections in the GUI, the first one is “Analysis” contains the LFR models in “Model”, in “Method” three methods for resolution are given, “Region definition” the region that will be analyzed, and “Approach” which contains all functions called during the analysis as “Progressive” or “Adaptive” and the type of “Lyapunov Functions”. The second is the “Results” stores the results data. Furthermore, the GUI has access to the LFR Toolbox, and to the YALMIP SDPT3.7.

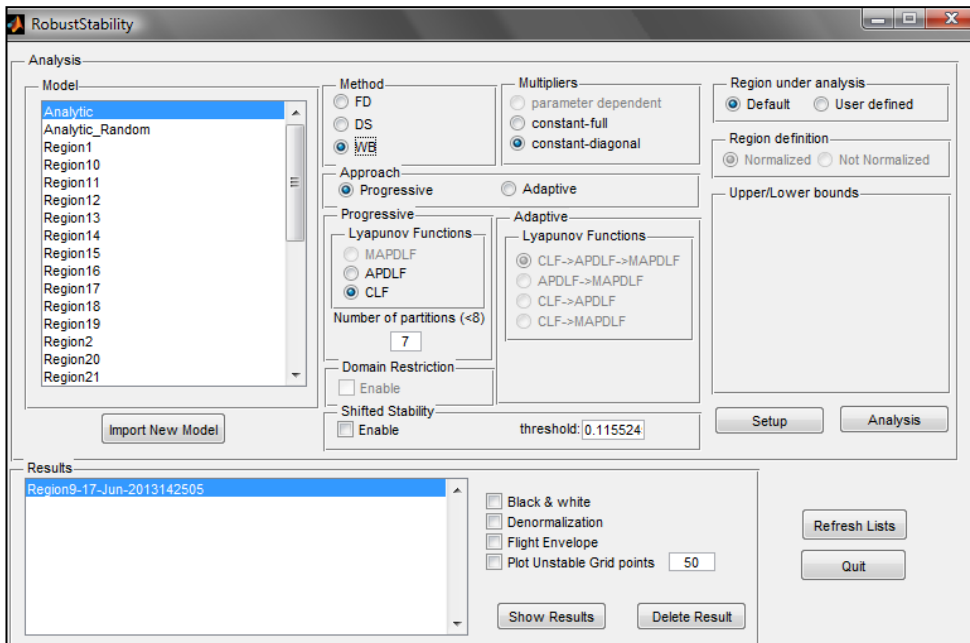


Figure 2. Robust Stability Toolbox

To perform the stability analysis, the obtained LFR model is firstly selected, and secondly one of the analysis parameters methods Fu-Dasgupta (FD), Dettori-Scherer (DS), and Wang-Balakrishnan (WB) is used. The theory of the Wang-Balakrishnan (WB) method is chosen, as it regards the normalization of the selected region. Other options exist such as the choice of the discretization number, the Lyapunov functions’ shape. After these parameters are validated, the stability analysis can be done for the selected region of the flight envelope.

5. ANALYSE OF RESULTS

5.1 LFR Results Validation

The results generated by LFR models must be evaluated [13]. To assess the accuracy of these results outside our interpolated points any number of points can be randomly generated, we have chosen 40 as an example, were randomly created from our interpolations, and they were compared with our reference points (representing the four (4) vertices of the region), for the 26 regions, we obtained 40 points for each of region.

It can be ensured that the interpolated points have a relative proximity with those references points, and remain in the area formed by these reference points. Figure 3 shows the eigenvalues results (imaginary versus real eigenvalues) for a given Xcg location and for 9 medium altitudes (regions 10 to 18), while Figure 4 gives the eigenvalues results for the highest altitudes (regions 24 and 25), while the results obtained for the other regions are given in Appendix. Only the positive side of the imaginary axis is shown in these symmetrical figures. Each pole pair is represented by a cross and circles.

The color “blue” is associated with the points used as reference points, and the “red” color indicates the randomly-generated interpolated points.

It can be observed that the quality of the interpolations is satisfied for the whole flight envelope, with the exception of the two regions (24 and 25) where it might be a problem for some Xcg locations. Indeed, at high altitudes, as shown in Figure 4, the interpolation of points seems to be more delicate and the pole pairs associated with the randomly-generated matrices appear to show some signs of disparity with the reference points, as indicated in Figure 4.

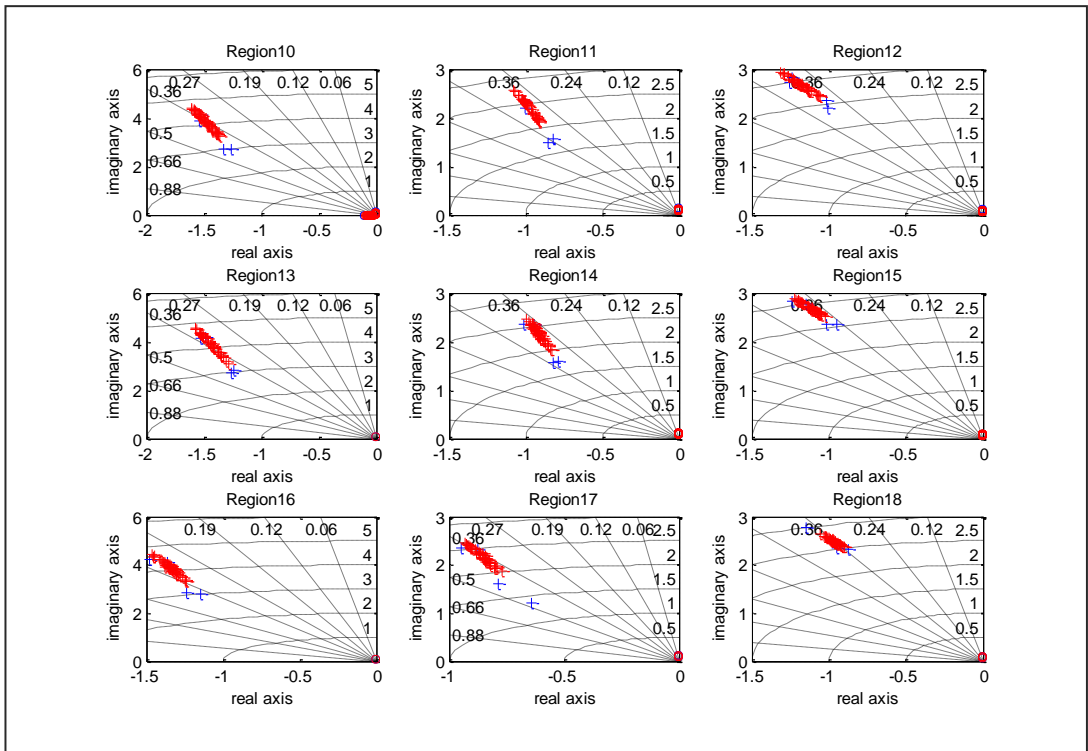


Figure 3. Comparison of eigenvalues for interpolated flight points with the reference values for medium altitudes (between 15,000 ft and 30,000 ft)

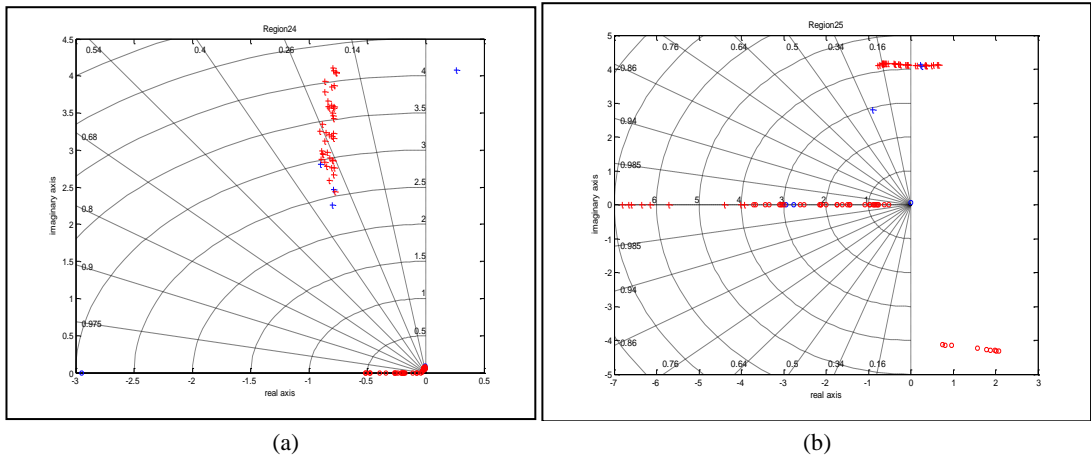


Figure 4. Comparison of eigenvalues for the interpolated flights points with the reference values at the highest altitudes (between 35,000 ft and 40,000 ft)

This dissimilarity is most critical for region 25, which has isolated poles represented by circles and red crosses, especially in its lower right corner and on its pure real axis in Figure 4(b). Regarding region 24 shown in Figure 4(a), two poles seem isolated from the rest of the poles.

Even though the results obtained for the other Xcg locations are not presented here, these results are of a similar type for the remaining 11 weight/Xcg configurations.

After analyzing all graphs, the quality of these results allows us to validate the interpolations made over our entire flight envelope for all Xcg locations, except for regions 24 and 25 at the highest altitudes.

Those results still need to be analyzed, but they will be considered “less reliable” if inconsistencies persist.

5.2 Stability Analysis Results

The interface allows the number of times that the region will be sub-divided to be freely selected in the analysis.

Whenever a region is discretized, it is sub-divided in four smaller sub-regions; each sub-region is analyzed, and possibly discretized at its turn, and so on until the 7th order of discretization.

This choice directly influences the results’ accuracy, but it also affects the execution time.

A compromise between the quality and the quantity of results had to be found. We have chosen to discretize a single region having a very high instability.

A first analysis was launched that allowed the maximum possible discretization, which was seven (7), which meant that the uncertainty domain (region) was going to be bisected 7 times representing potentially $2^7 = 128$ tiles per side.

For a model with 2 uncertainties, the region (uncertainty domain) was meshed a number of $2^7 \times 2^7 = 16,384$ tiles, which meant, that the region was subdivided in 4 sub-regions each time until reaching the 7 times, that was equivalent to $\sum_{k=0}^7 4^k = 16,384$ tiles, that were obtained in the worst cases (in the proximity of instability). The results analyses are presented in Figure 5 and Figure 6.

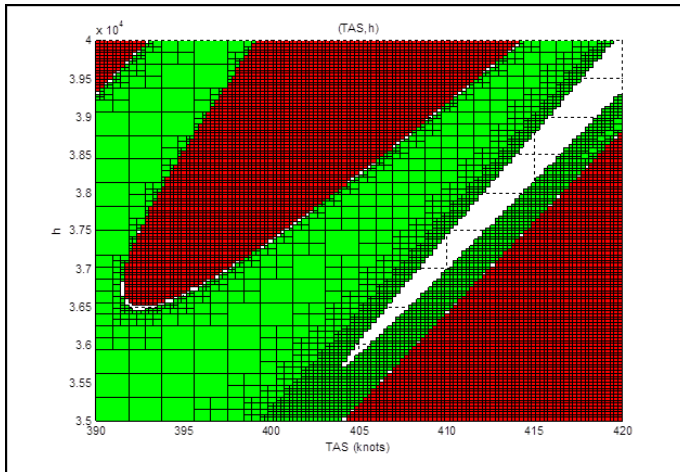


Figure 5. Results for the single region with 7th order discretization (altitude =35,000ft -40,000 ft and TAS= 390 – 420 knots)

```

Model: Region26_inter09-Sep-2013
Method: WB
Relaxation: Constant diagonal multipliers
Candidate Lyapunov function: CLF
Weak Stability analysis disabled
Partitioning: 7

Approach: Progressive

Flight Envelope restriction: Disabled

Region defined in the normalized space.
-----
Region:
 [ Lower bound , Upper bound ]
Vitesse [ -1 , 1 ]
h [ -1 , 1 ]
-----
Results:
-----

```

NOPs	Time (h:m:s)	Time/OP (h:m:s)	Time (Gridding) (h:m:s)	Time/partition (Gridding) (h:m:s)
4555	0:57:39	0:0:0	0:3:2	0:0:0

Cleared (%)	Unstable (%)	Unknown (%)	Rate (%)
49.50562	44.43359	6.06079	89.09271

Figure 6. Results of a completed stability analysis

Figure 6 and Figure 8 show the results when a region’s analysis has been completed by 7th and 5th order discretization, respectively. These figures obtained using the Matlab command summarize the information about the region; in fact the method selected, the candidate Lyapunov function, the approach, the order of discretization, and the bounds of the normalized uncertainties used in the LFR model are indicated. The results represent the Number of Optimizations denoted by NOPs that have been solved (they correspond to the

number of tiles attempted to be cleared, that is expressed by the sum of the number of the “green” plus the number of “red” tiles) [6], therefore to the time taken for the region analysis. These results are presented graphically in Figures 5 and 7, where they indicate the sub-regions where the analysis has been cleared; the stable sub-regions were in “green”, the unstable sub-regions were in “red”, and the unknown sub-regions were in “white”; when the sub-regions (tiles) are unknown so denoted in “white”, the aircraft cannot be trimmed for its corresponding altitudes h and TAS ; the results were expressed in percentages (%) of the area of the analyzed region in Figures 5 and 7. The “Rate” value indicates the ratio of the cleared (the stable (green) plus the unstable (red)) part to the neutral “white” part of the region.

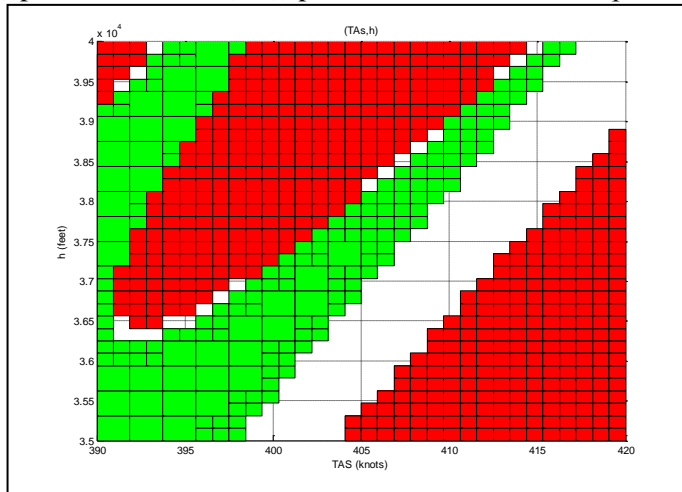


Figure 7. Region with 5th order discretization (altitude= 35,000ft -40,000 ft and TAS 390 – 420 knots)

```

Analysis completed
-----
Model: Region26_inter09-Sep-2013
Method: WB
Relaxation: Constant diagonal multipliers
Candidate Lyapunov function: CLF
Weak Stability analysis disabled
Partitioning: 5

Approach: Progressive

Flight Envelope restriction: Disabled

Region defined in the normalized space.

-----
Region:
[ Lower bound , Upper bound ]
Vitesse  [ -1 , 1 ]
h        [ -1 , 1 ]

-----
Results:
-----

```

NOPs	Time (h:m:s)	Time/OP (h:m:s)	Time (Gridding) (h:m:s)	Time/partition (Gridding) (h:m:s)
509	0:7:58	0:0:0	0:0:15	0:0:0

Cleared (%)	Unstable (%)	Unknown (%)	Rate (%)
28.71094	49.41406	21.87500	56.75676

Figure 8. Results of 5th order discretization of the region

Four hours took to complete the computations need for the results analysis. The 26 LFR models defined by interpolation for 12 weight/Xcg configurations have been analyzed for the stability of the longitudinal aircraft model. These results indicated that it was not necessary to obtain a very high discretization order of the regions' subdivisions. 7th order discretization results were obtained for “2” uncertainties $2^7 = 128$ maximum tiles per side. Given the fact that the largest region defined in Figure 5 is 80 knots wide and 5,000 ft high, and that a tile precision is represented by 0.625 knots and 39.06 ft, then a computation time of almost 57 min is required to analyze the entire region, and to solve 4555 (NOPs) optimizations for this region (this number was computed by the Stability Analysis software which represents the sum of the stable and the unstable sub-regions or “tiles”).

The system discretization was reduced from the 7th order to a 5th order as shown in Figure 7, which means that a maximum resolution of 2.5 knots and 156.25 ft per region was applied. This discretization reduced highly the computing time for the region from 57 min in its 7th order of discretization (Figure 6) to almost 8 min in its 5th order of discretization, the time that takes to analyze the entire region, and to solve 509 (NOPs) optimizations (this number was computed by the Stability Analysis software which represents the sum of the stable and the unstable sub-regions or “tiles”) as shown in Figure 8. The results produced by the 7th order discretization are of course better than those obtained from a 5th order discretization, especially in terms of “Rate”.

The rate of 6.06% is obtained in the 7th order discretization while the rate of 21.87% is obtained in the 5th order discretization, which means that the unknown area in the region with 5th order discretization is larger than in the region with 7th order of discretization. The computing time was used to choose between these two orders of discretization. The studies considering discretization of up to $2^5 = 32$ elements per variation range of each uncertainty (h , and TAS) were carried out, and seemed to be a very good compromise for the Cessna Citation X stability analysis due to its “very good natural stability”.

5.3 Results of the Longitudinal Flight Envelope Stability Analysis

Figures 9 and 10 show the stability analysis results obtained for two different weight and Xcg positions using the Wang-Balakrishnan method based on the Lyapunov constant functions, and the 5th order discretization.

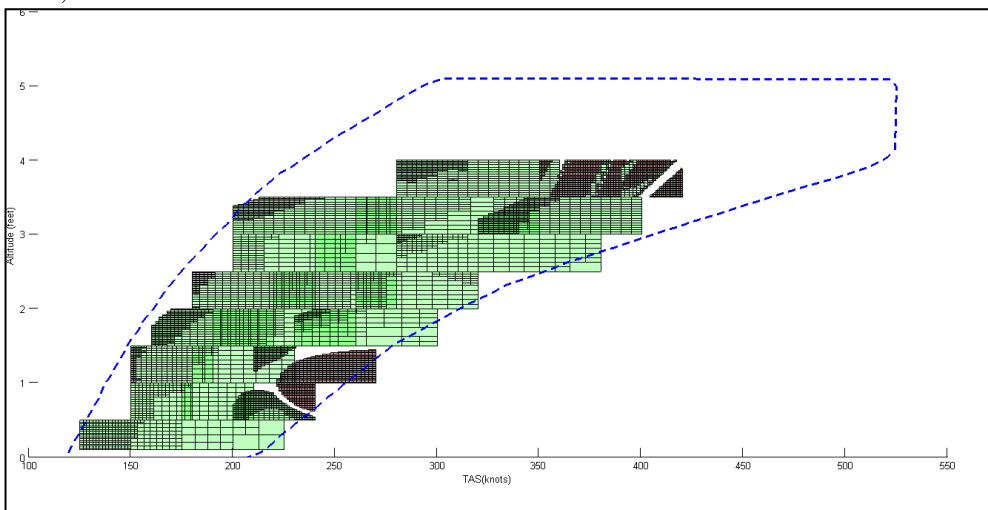


Figure 9. Stability analysis of a longitudinal model for 1st weight/Xcg configuration (24000lbs/30%)

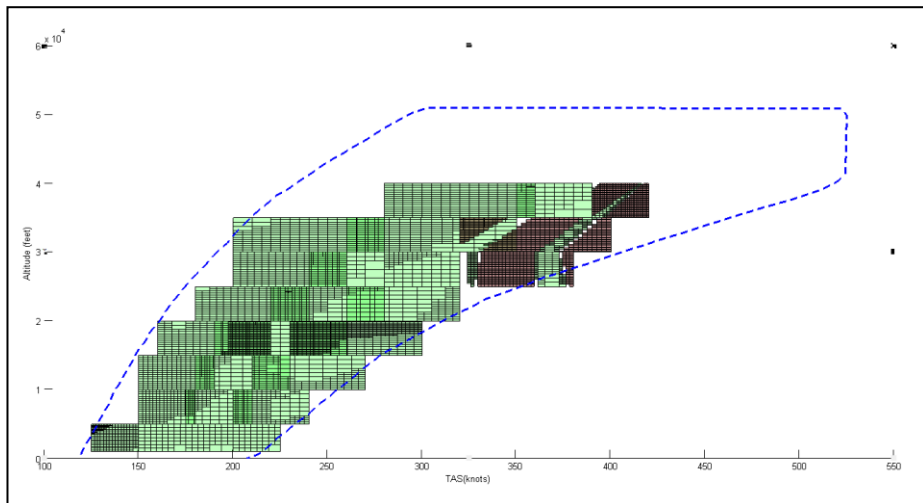


Figure 10. Stability analysis of a longitudinal model for 7th weight/Xcg configuration (28000lbs/30%)

Firstly, the continuity between regions is found. Indeed, the instability zone, located for low altitude and average speed that is shown in Figure 9 covers two distinct regions, and therefore two different interpolated models. The “red” area stops at the border between the two models, and this is marked for unstable regions. Figure 10 illustrates this fact by revealing a peak discretization on the back of the flight envelope and along the stall limit from the lowest to the highest altitude. Secondly, some conflicts are discussed that appear in the superposed regions. The results of these recovering areas are not consistent, and are sometimes contradictory. The regions are not only built by interpolating, but also by extrapolating data for the left upper and the right lower peaks. In all cases, “incoherence” is caused by extrapolation; the model does not describe the reality accurately. Therefore, the area(s) presenting an extrapolation situation must be neglected.

6. CONCLUSION

The aim of the clearance process was to demonstrate that a set of selected criteria expressing desired stability and handling requirements was fulfilled in the presence of all possible sources of uncertainties. The stability criterion can be reformulated to be a clearance criterion, as mentioned by Airbus and can be classified in four classes: 1) the aeroelastic stability, 2) turbulence, 3) comfort, and 3) maneuvers criteria. Only the eigenvalue stability known as (aeroelastic stability) envelope criterion was presented for the longitudinal Cessna Citation X business aircraft in the open loop system, which was the basis for any Cessna Citation X flight controller design validation and clearance.

The longitudinal eigenvalue stability (open loop system without a controller) has been made for the 26 interpolated regions, and it was also a very good tool for validating the LFR models generated by the LFR GUI in Part1. The analysis indicated the regions reliability in representing the aircraft dynamics in its whole envelope for all its uncertainty parameters values. This analysis highlighted the importance of the work that was performed for the exploitation of results in this research. The only disadvantage of this method was that it was still requires a relatively long time calculation, of almost four hours for the entire flight envelope. However, practical aspects of this study were considered in the aircraft stability analysis, by using the low order discretization's. In this paper, 5th order discretization was applied. Future work will evaluate the eigenvalue stability of the Cessna Citation X

longitudinal closed loop aircraft model by using H -infinity, and optimal controllers developed during earlier researches [8],[34]-[36] to show if the interaction of the flight controller with the Cessna Citation X would induce any instability.

ACKNOWLEDGEMENTS

This work was performed at the LARCASE (Laboratory of active controls, avionics and aeroservoelasticity research). We would like to thank to the project leader Mr Ken Dustin and his team at CAE Inc. for their support in the development of the Aircraft Research Flight Simulator at the LARCASE laboratory.

This simulator was obtained thanks to research grants that were approved by the Canada Foundation for Innovation (CFI) and the Ministère de Développement de l'Économie, de l'Innovation et de l'Exportation MDEIE. In addition, this research was funded by the Natural Sciences and Engineering Research Council of Canada NSERC in the frame of Canada Research Chair Programs; Dr Ruxandra Botez is Canada Research Chair Holder in Aircraft Modeling and Simulation Technologies. Thanks are also due to Mrs Odette Lacasse and Mr Oscar Carranza at ETS for their continuing enthusiasm and support.

REFERENCES

- [1] C. Fielding, A.Varga, S. Bennani, M. Selier, *Advanced Techniques for Clearance of Flight Control Laws*, Springer Science & Business Media, 2002.
- [2] M. Selier, C. Fielding, U. Korte, R. Luckner, New Analysis Techniques for Clearance of Flight Control Laws, An overview of GARTEUR Flight Mechanics Action Group 11, NLR-TP-2004, 147, *AIAA Guidance, Navigation and Control Conference*, Austin, TX, USA, 11-14 August, 2003.
- [3] R. F. De Oliveira, G. Puyou, On the Use of Optimization for Flight Control Laws Clearance: a Practical Approach, *18th IFAC World Congress Proceedings*, Milano, Italy, August 28-September 2, Vol. **44**, No. 1, pp. 9881-9886, 2011.
- [4] P. Goupil, G. Puyou, A high Fidelity AIRBUS Benchmark for System Fault Detection and Isolation and Flight Control Law Clearance, *Progress in Flight Dynamics, GNC, and Avionics*, Vol. **6**, pp. 249-262, DOI: 10.1051/eucass/201306249, 2013.
- [5] Y. Boughari, R. M. Botez, F. Theel, G. Ghazi, Optimal Flight Control on Cessna X Aircraft using Differential Evolution, *IATED Modelling, Simulation Identification and Control Conference (MIC 2014)*, Innsbruck, Austria, February 17-19, doi: 10.2316/P.2014.809-052, 2014.
- [6] Y. Boughari, R. M. Botez, G. Ghazi, F. Theel, Evolutionary Algorithms for Robust Cessna Citation X Flight Control, Paper No. 2014-01-2166, *SAE 2014 Aerospace Systems and Technology Conference*, Cincinnati, Ohio, USA, September 23-25, doi:10.4271/2014-01-2166, 2014.
- [7] Y. Boughari, R. M. Botez, Optimal Flight Control on the Hawker 800 XP Business Aircraft, *IECON 2012 - 38th Annual Conference on IEEE Industrial Electronics Society Proceedings*, Montreal, Que., Canada, October 25-28, pp. 5471-5476, DOI: 10.1109/IECON.2012.6388953, 2012.
- [8] Y. Boughari, R. M. Botez, G. Ghazi, F. Theel, Flight Control Clearance of the Cessna Citation X using Evolutionary Algorithms, *Proceedings of the Institution of Mechanical Engineers (IMEchE), Part G: Aerospace Engineering*, doi: 10.1177/0954410016640821, 2016.
- [9] G. Ghazi, R. M. Botez, Lateral Controller Design for the Cessna Citation X with Handling Qualities and Robustness Requirements. *62nd Canadian Aeronautical Society Institute CASI Aeronautics Conference and AGM & 3rd GARDN Conference Proceeding*, Montreal, Que., Canada, 19-21 May, 2015.
- [10] G. Ghazi, R. M. Botez, *New Robust Control Analysis Methodology for Lynx Helicopter and Cessna Citation X Aircraft Using Guardian Maps, Genetic Algorithms and LQR Theories Combinations*, AHS 70th Annual Forum & Technology Display Proceedings, Montreal, Quebec, Canada, 20-22 May 20-22, 2014.
- [11] A. Varga, *Clearance Criteria for Civil Aircraft*, COFCLUO, AST5-CT-2006-030768, Specific Targeted Research report, pp. 1-28, 2010.
- [12] C. Favre, Fly-By-Wire for Commercial Aircraft: the Airbus Experience, *International Journal of Control*, Vol. **59**, No. 1, pp.139-157, 1994.
- [13] A. Varga, A. Hansson, G. Puyou, *Optimization Based Clearance of Flight Control Laws*, Lecture Notes in Control and Information Science, Springer Edition, pp. 121, 2012.

- [14] D. H. Baldelli, R. Lind, M. Brenner, Nonlinear Aeroelastic/Aeroservoelastic Modeling by Block-Oriented Identification, *Journal of Guidance, Control, and Dynamics*, Vol **28**, No 5, pp. 1056-1064, 2005.
- [15] N. Anton, R. M. Botez, Weight Functions Method for Stability Analysis applied as Design Tool for Hawker 800XP Aircraft, *The Aeronautical Journal*, Vol. **119**, No. 1218, pp. 981-999, 2015.
- [16] N. Anton, R. M. Botez, D. Popescu, Application of the Weight Function Method on a High Incidence Research Aircraft Model, *The Aeronautical Journal*, Vol. **117**, No. 1195, pp. 897-912, 2013.
- [17] G. Ghazi, R. M. Botez, Development of a High-Fidelity Simulation Model for a Research Environment, *SAE Technical Paper*, 22-24 September, 2015.
- [18] G. Ghazi, *Développement d'une lateforme de simulation et d'un pilote automatique-application aux Cessna Citation X et Hawker 800XP*, Doctoral dissertation, Master's thesis, University of Quebec-École Polytechnique de Montréal, doi: 10.13140/2.1, 2014.
- [19] A. Garulli, A. Masi S. Paoletti, E. Turkoglu, *LFR_RAI User's Guide*, March 3, pp. 1-28, available at http://www.dii.unisi.it/~garulli/lfr_rai.
- [20] C. Poussot-Vassal, C. Roos, Generation of a Reduced-Order LPV/LFT Model from a set of Large-Scale MIMO LTI Flexible Aircraft Models, *Control Engineering Practice*, September 30, Vol. **20**, No. 9, pp. 919-930, 2012.
- [21] R. C. Nelson, *Flight Stability and Automatic Control*, McGraw Hill Education, 1998.
- [22] M. Johansson, A. Rantzer, Computation of Piecewise Quadratic Lyapunov Functions for Hybrid Systems, *IEEE Transactions on Automatic Control*, Vol. **43**, No. 4, pp. 555-559, 1998.
- [23] W. J. Rugh, *Linear System Theory*, Vol **2**, Upper Saddle River, NJ: Prentice Hall Edition, 1996.
- [24] A. Papachristodoulou, S. Prajna, On the construction of Lyapunov Functions using the Sum of Squares Decomposition, *Proceedings of the 41st IEEE Conference on Decision and Control*, December 10, Vol. **3**, pp. 3482-3487, 2002.
- [25] V. L. Kharitonov, A. P. Zhabko, Lyapunov-Krasovskii Approach to the Robust Stability Analysis of Time-Delay Systems, *Automatica*, January 31, Vol. **39**, No. 1, pp. 15-20, 2003.
- [26] M. Corless, *Robust Stability Analysis and Controller Design with Quadratic Lyapunov Functions, Variable Structure and Lyapunov Control*, Vol. **193** of the series Lecture Notes in Control and Information Sciences, pp. 181-203, Springer Berlin Heidelberg Edition, 2005.
- [27] H. Lin, P. J. Antsaklis, Stability and Stabilizability of Switched Linear Systems: a Survey of Recent Results. *IEEE Transactions on Automatic Control*, Vol. **54**, No. 2, pp.308-322, 2009.
- [28] J. Löfberg, *YALMIP: A Toolbox for Modeling and Optimization in MATLAB*, IEEE International Symposium on Computer Aided Control Systems Design, Tapei, Taiwan, September 4, pp. 284-289, 2004.
- [29] K. C. Toh, M. J. Todd, R. H. Tütüncü, *On the Implementation and usage of SDPT3—a Matlab Software Package for Semidefinite-Quadratic-Linear Programming*, version 4.0 Handbook on Semidefinite, Conic and Polynomial Optimization, pp. 715-754, Springer Edition, USA, 2012.
- [30] A. Garulli, A. Masi, S. Paoletti, E. Türkoglu & C. Roos, *D2. 3.5 Final Report WP2. 3*, 2010, available at http://www.dii.unisi.it/~garulli/lfr_rai/D2.3.5.pdf.
- [31] F. Wang, V. Balakrishnan, Improved Stability Analysis and Gain-Scheduled Controller Synthesis for Parameter-Dependent Systems, *IEEE Transactions on Automatic Control*, Vol. **47**, No. 5, pp. 720-34, 2002.
- [32] M. Dettori, C. W. Scherer, New Robust Stability and Performance Conditions Based on Parameter Dependent Multipliers, *Proceedings of the 39th IEEE Conference on Decision and Control*, Vol. **5**, pp. 4187-4192, 2000.
- [33] M. Fu, S. Dasgupta, Parametric Lyapunov Functions for Uncertain Systems: *The Multiplier Approach, Advances in Linear Matrix Inequality Methods in Control*, pp. 95-108, 2000.
- [34] Y. Boughari, G. Ghazi, R. M. Botez, F. Theel, New Methodology for Optimal Flight Control Using Differential Evolution Algorithms Applied on the Cessna Citation X Business Aircraft - Part 1. Design and Optimization, *INCAS BULLETIN*, Vol. **9**, Issue 2, (online) ISSN 2247-4528, (print) ISSN 2066-8201, ISSN-L 2066-8201, pp. 31-44, DOI: 10.13111/2066-8201.2017.9.2.3, 2017.
- [35] Y. Boughari, G. Ghazi, R. M. Botez, F. Theel, New Methodology for Optimal Flight Control using Differential Evolution Algorithms applied on the Cessna Citation X Business Aircraft - Part 2. Validation on Aircraft Research Flight Level D Simulator, *INCAS BULLETIN*, Vol. **9**, Issue 2, (online) ISSN 2247-4528, (print) ISSN 2066-8201, ISSN-L 2066-8201, pp. 45-59, doi: 10.13111/2066-8201.2017.9.2.4, 2017.
- [36] Y. Boughari et al. Optimal Control New Methodologies Validation On the Research Aircraft Flight Simulator of the Cessna Citation X Business Aircraft, *Internationa Journal of Contemporary Energy*, Vol **3**, No. 1, doi: 10.14621/ce.20170102, 2017.